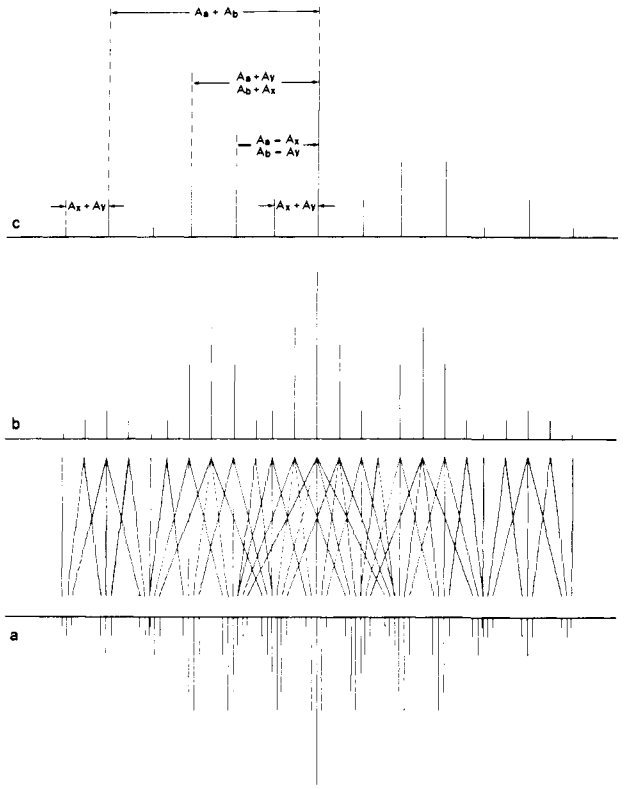

Figure 2. Stick diagram reconstructions of the 9,10-octalin oxide radical cation **1** spectra for (a) slow, (b) fast, and (c) intermediate rates of exchange between $2H_a$ and $2H_b$ and between $2H_x$ and $2H_y$. The intensities of the line components in stick plot b are shown at half scale, and the lines connecting the components in plots a and b show the correlations between nuclear spin states.

2. Thus, the 140-K spectrum in Figure 1 corresponds to the 13 line groups for the rigid-limit spectrum in plot a, while the coalescence spectrum at 160 K fits the reconstruction in plot c of line components whose resonances remain unaltered by exchange (plots a and b). Simulations of the temperature-dependent spectra were made by using the modified Bloch equations for a two-jump model,[23] and the interconversion rate constants used to obtain the fits in Figure 1 obeyed an Arrhenius relation with $A = 5.6 \times 10^{12}$ s^{-1} and $E_a = 3.66$ kcal mol^{-1}. These parameters are very similar to those reported for ring inversion in the cyclohexyl radical[25] and the cyclohexanesemidione radical anion.[26]

An obvious corollary is that dynamic effects should be absent in the rigid cation of *syn*-sesquinorbornene oxide (**2**). In

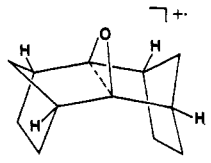

2

agreement, its ESR spectrum showed no temperature dependence and consisted of a quintet from coupling to the four equivalent bridgehead hydrogens (Table I). Together with the absence of significant *g*-anisotropy for both **1** and **2**, the detection of angular-dependent couplings for hydrogens in β positions with respect to the oxirane ring carbons strongly supports the assignment to carbon-centered rather than oxygen-centered cations. Although high-level ab initio MO calculations predict a $^2B_1$ ground state rather than the analogous carbon-centered $^2A_1$ state for the ring-closed parent oxirane cation,[19] the change in the state ordering on going to these rigid species is attributable to the effect of alkylation which is known to destabilize the a_1 relative to the b_1 orbital in methylated oxiranes.[27]

In fact, AM1 calculations[28] confirm that **1** possesses a ^2A ground state with transoid C_2 symmetry. Moreover, the calculated dihedral angles for the optimized geometry are in excellent agreement with those deduced from the ESR analysis (Table I). Also, the AM1 calculations reveal that the spin density is largely concentrated in the 2p orbitals of the α-carbons[29] which assume a nearly planar configuration with a highly elongated C_α–C_α' bond distance of 2.21 Å. Clearly, the C–C bond must be very weak in these intermediate CC(σ) species, and their observation is probably only feasible when rotation about the C–O bonds to the more stable oxallyl radical cation[8-10,16-19] is prohibited, as by the bicyclic ring systems in the present case.

Acknowledgment. Support of this research at the University of Tennessee was provided by the Division of Chemical Sciences, U.S. Department of Energy (report no. DOE/ER/02968-171). The support of the Schweizetischer Nationalfonds (Project No. 2.044–0.86) is also gratefully acknowledged.

Supplementary Material Available: Figure showing the ESR spectrum of the *syn*-sesquinorbornene oxide cation in the $CFCl_3$ matrix (1 page). Ordering information is given on any current masthead page.

(25) Ogawa, S.; Fessenden, R. W. *J. Chem. Phys.* **1964**, *41*, 994.
(26) Russell, G. A.; Underwood, G. R., Lini, D. C. *J. Am. Chem. Soc.* **1967**, *89*, 6636.
(27) (a) McAlduff, E. J.; Houk, K. N. *Can. J. Chem.* **1977**, *55*, 318. (b) The photoelectron spectra of tetraalkylated oxiranes indicate that the adiabatic ionization leading to the $^2A_1$ state may occur at lower energy than that yielding the $^2B_1$ state.[12]
(28) Dewar M. J. S.; Zoebisch, E. G.; Healy, E. F.; Stewart, J. J. P. *J. Am. Chem. Soc.* **1985**, *107*, 3902.
(29) Both AM1 and INDO calculations on the ^2A state of **1** in the optimized geometry indicate that very little spin density (ρ ca. 0.02–0.05) resides in the symmetry-adapted sp orbital on oxygen, as expected because this s-rich orbital is of lower energy and overlaps poorly with the in-plane p orbitals on the α-carbons which carry most of the spin density. Thus the singly occupied a orbital can be considered as delocalized between the two α-carbons mainly through space rather than through the C–O bonds or the oxygen lone-pair (n) orbital.

Voltammetric Studies of the Interaction of Tris(1,10-phenanthroline)cobalt(III) with DNA

Michael T. Carter and Allen J. Bard*

Department of Chemistry, The University of Texas Austin, Texas 78712

Received July 7, 1987

We report here how the changes in the cyclic voltammetric (CV) behavior of tris(1,10-phenanthroline)cobalt(III), Co(phen)$_3^{3+}$, in an aqueous medium upon addition of DNA can be used to probe the interaction between these species. Coordination complexes of 1,10-phenanthroline and 4,7-diphenyl-1,10-phenanthroline with Ru(II) and Co(III),[1,2] and other metal chelates[3-6] that intercalate between the stacked base pairs of native

(1) (a) Barton, J. K.; Danishefsky, A. T.; Goldberg, J. M. *J. Am. Chem. Soc.* **1984**, *106*, 2172. (b) Barton, J. K.; Basile, L. A.; Danishefsky, A. T.; Alexandrescu, A. *Proc. Natl. Acad. Sci. U.S.A.* **1984**, *81*, 1961. (c) Kumar, C. V.; Barton, J. K.; Turro, N. J. *J. Am. Chem. Soc.* **1985**, *107*, 5518. (d) Barton, J. K.; Goldberg, J. M.; Kumar, C. V.; Turro, N. J. *J. Am. Chem. Soc.* **1986**, *108*, 2081. (e) Mei, H.-Y.; Barton, J. K. *J. Am. Chem. Soc.* **1986**, *108*, 7414. (f) Barton, J. K. *J. Biomol. Struct. Dyn.* **1981**, *1*, 621. (g) Goldstein, B. M.; Barton, J. K.; Berman, H. M. *Inorg. Chem.* **1986**, *25*, 842.
(2) (a) Barton, J. K.; Dannenberg, J. J.; Raphael, A. L. *J. Am. Chem. Soc.* **1982**, *104*, 4967. (b) Barton, J. K.; Lolis, E. *J. Am. Chem. Soc.* **1985**, *107*, 708.
(3) Hecht, S. M. *Acc. Chem. Res.* **1986**, *19*, 383.
(4) Subramanian, R.; Meares, C. F. *J. Am. Chem. Soc.* **1986**, *108*, 6427.
(5) Goldstein, S.; Czapski, G. *J. Am. Chem. Soc.* **1986**, *108*, 2244.

0002-7863/87/1509-7528$01.50/0

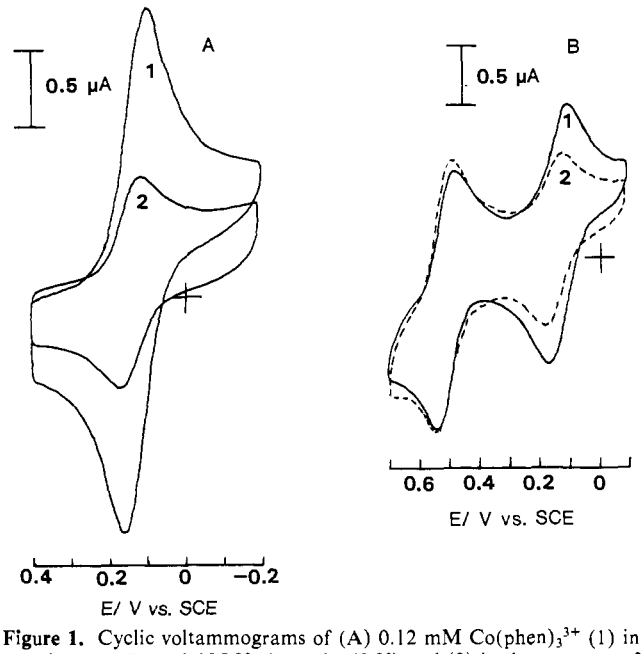

Figure 1. Cyclic voltammograms of (A) 0.12 mM $Co(phen)_3^{3+}$ (1) in the absence (E_{pc} = 0.095 V, E_{pa} = 0.160 V) and (2) in the presence of DNA (5.3 mM nucleotide phosphate) (E_{pc} = 0.115 V; E_{pa} = 0.175 V) and (B) 0.10 mM $Co(phen)_3^{3+}$ + 0.11 mM $Mo(CN)_8^{4-}$ (1) in the absence and (2) in the presence of 4.8 mM nucleotide phosphate. Supporting electrolyte, 50 mM NaCl, 5 mM Tris, pH 7.1. Sweep rate, 100 mV/s. Glassy carbon-working electrode (0.07 cm^2). All potentials reported vs saturated calomel electrode (SCE).

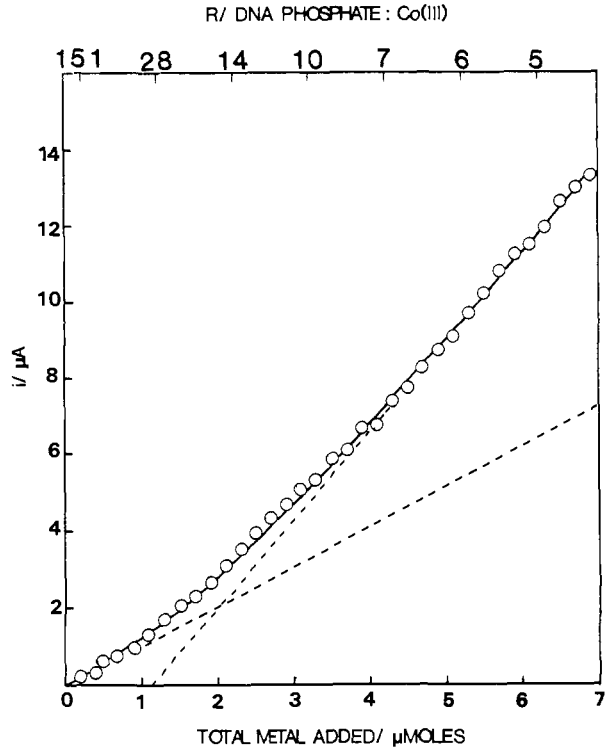

Figure 2. CV peak current for total Co(III) reduction for 3.02 × 10^{-5} mol nucleotide phosphate titrated with 1.0 mM $Co(phen)_3^{3+}$. Initial solution volume 5 cm^3. Other conditions as in Figure 1. Solid curve represents the results for best fit parameters as given in text. Straight lines are the limiting slopes.

DNA, have been actively investigated as probes of DNA structure in solution and as stereoselective or conformation-specific agents for the photoactivated cleavage of DNA.[7]

The nature of the interaction between these metallointercalation agents and DNA has primarily been studied by spectroscopic and X-ray crystallographic methods.[8] While electrochemical investigations of DNA, via the reduction of the purine and pyrimidine bases, have been carried out,[9] to our knowledge, no such studies of metallointercalation agents in the presence of double-stranded DNA have been published. Electrochemical studies of transition-metal complexes, e.g., of phen,[10] have been extensive, and the effect of ligand concentration on potential can be used to determine formation constants. Thus electrochemical investigations of metal–DNA interactions can provide a useful complement to spectroscopic methods, e.g., for nonabsorbing species, and yield, as shown below, information about interactions with both the reduced and oxidized form of the metal.

Typical CV behavior of $Co(phen)_3^{3+}$ [11] in the absence (curve 1) and presence (curve 2) of calf thymus DNA[12] is shown in Figure 1a. The addition of an excess of DNA causes the peak currents of the CV waves for reduction of $Co(phen)_3^{3+}$ to the 2+ form and anodic wave on the reverse scan to diminish considerably. The cathodic peak current, i_{pc}, shown in curve A2, decreased to ca. 40% of that in the absence of DNA. Additionally, the peak potentials, E_{pc} and E_{pa}, both shifted to more positive values, equivalent to a shift in the formal potential of the $Co(phen)_3^{3+/2+}$ couple, $E^{0'}$ (taken as the average of E_{pc} and E_{pa}), of 17 mV. The limiting shift of the polarographic $E_{1/2}$ by differential pulse voltammetry was 40 mV, in the presence of a very large excess of DNA. The peak potential separations ($\Delta E_p = |E_{pc} - E_{pa}|$) and peak shapes, $|E_{pc} - E_{p/2}|$, were between 60–65 mV, independent of DNA phosphate concentration and potential sweep rate ($5 \leq v \leq 200$ mV s^{-1}) indicating a reversible $1e^-$ redox process. In all cases i_p was a linear function of $v^{1/2}$, as expected for a diffusion controlled process, and $i_{pa}/i_{pc} = 1$ at all v and concentrations of DNA.

To show that the decrease in i_{pc} is due to binding of $Co(phen)_3^{3+}$ to the large, slowly diffusing DNA and not to an increase in solution viscosity,[13] we performed CV experiments on a mixture of $Co(phen)_3^{3+}$ (0.1 mM), which intercalates between the DNA base pairs[7b] and $Mo(CN)_8^{4-}$ (0.11 mM), which, because of its negative charge, should not interact with DNA. In the absence of DNA (Figure 1b), well-defined waves for the free $Mo(CN)_8^{4-/5-}$ ($E^{0'}$ = 0.51 V) and $Co(phen)_3^{3+/2+}$ ($E^{0'}$ = 0.13 V) couples are evident (curve B1). Upon addition of an excess of nucleotide phosphate (curve B2), $E^{0'}$ and i_{pc} changed as described previously (curve A). The $E^{0'}$ of $Mo(CN)_8^{4-/5-}$ was essentially unaffected by the addition of DNA, and the ratio of the cathodic peak currents, corrected for the background current, which increased upon DNA addition, before and after DNA addition was ca. 0.90. Thus, the small perturbation in the $Mo(CN)_8^{4-/5-}$ waves by the

(6) (a) Jennette, K. W.; Lippard, S. J.; Vassiliades, G. A.; Bauer, W. R. *Proc. Natl. Acad. Sci. U.S.A.* **1974**, *71*, 3839. (b) Wang, A. H. J.; Nathans, J.; van der Marel, G.; van Boom, J. H. *Nature (London)* **1978**, *276*, 471. (c) Lippard, S. J.; Bond, P. J.; Wu, K. C.; Bauer, W. R. *Science (Washington, D.C.)* **1976**, *194*, 726.

(7) (a) Barton, J. K.; Raphael, A. L. *Proc. Natl. Acad. Sci. U.S.A.* **1985**, *82*, 6460. (b) Barton, J. K.; Raphael, A. L. *J. Am. Chem. Soc.* **1984**, *106*, 2466. (c) Barton, J. K.; Paranawithana, S. R. *Biochemistry* **1986**, *25*, 2205. (d) Barton, J. K. *Science (Washington, D.C.)* **1986**, *233*, 727. (e) Kelly, J. M.; Tossi, A. B.; McConnell, D. J.; OhUigin, C. *Nucl. Acids Res.* **1985**, *13*, 6017.

(8) Barton, J. K. *Comm. Inorg. Chem.* **1985**, *3*, 321.

(9) (a) Sequaris, J.-M.; Kaba, M. L.; Valenta, P. *Bioelectrochem. Bioenerg.* **1984**, *13*, 225. (b) Berg, H. In *Comprehensive Treatise of Electrochemistry*; Srinivasan, S., Chizmadzhev, Y. A., Bockris, J. O'M., Conway, B. E., Eds.; Plenum Press: New York, 1985; Vol. 10, Chapter 3. (c) Berg, H.; Fiedler, U.; Flemming, J.; Horn, G. *Bioelectrochem. Bioenerg.* **1985**, *14*, 417. (d) Paleček, E.; Jelen, F.; Trnková, L. *Gen. Physiol. Biophys.* **1986**, *5*, 315.

(10) Maki, N.; Tanaka, N. In *Encyclopedia of Electrochemistry of the Elements*; Bard, A. J., Ed.; Marcel Dekker: New York, 1975; Vol. 3, pp 43–210.

(11) Dollimore, L. S.; Gillard, R. D. *J. Chem. Soc., Dalton. Trans.* **1973**, 933.

(12) Calf thymus DNA (Sigma Chemical Co.) was purified by phenol extraction (Maniatis, T.; Fritsch, E. F.; Sambrook, J. *Molecular Cloning*; Cold Spring Harbor Laboratory, 1982).

(13) Marmur, J.; Rownd, R.; Schildkraut, G. L. In *Progress in Nucleic Acids Research*; Cohn, W. E., Ed.; Academic Press: New York, 1963; Vol. 1.

DNA can be attributed to an increase in solution viscosity, while the larger changes in both $E^{0'}$ and i_{pc} for $Co(phen)_3^{3+}$ are attributed to interactions with the DNA duplex.

CV experiments were carried out in which the ratio of DNA to $Co(phen)_3^{3+}$ was varied. The ratios are reported in terms of R = [nucleotide phosphate]/[cobalt(III)].[14] At $R = 0$, the diffusion coefficient of the free $Co(phen)_3^{3+}$, D_f, was obtained from the $i_p/v^{1/2}$ data ($5 \le v \le 200$ mV/s) as $(3.6 \pm 0.8) \times 10^{-6}$ cm^2/s. At $R = 304.5$, the apparent diffusion coefficient of the bound metal complex D_b, obtained by differential pulse voltammetry, was $(3.1 \pm 1.6) \times 10^{-7}$ cm^2/s.

A titration of 30.2 μmol nucleotide phosphate with $Co(phen)_3^{3+}$ while measuring the total cathodic peak current (i_T) as a function of μmol metal chelate added (C_T) (or R) gave the results shown in Figure 2. Two limiting regions are found. At large R the current is attributed primarily to $Co(phen)_3^{3+}$ intercalated to DNA (characterized by a concentration, C_b, and D_b), while at very small R the main contribution to i_T is free $Co(phen)_3^{3+}$ in solution (concentration, C_f and D_f). The total current at any R is

$$i_T = B[D_f^{1/2}C_f + D_b^{1/2}C_b] \quad (1)$$

where $B = 2.69 \times 10^5\ n^{3/2}\ Av^{1/2}$ for CV of a Nernstian wave at 25°.[16] C_b is related to the total metal added, C_T, with the assumption of control by the equilibrium binding of the chelate by DNA by

$$C_b = \{b - (b^2 - 2K^2C_T[NP]/n_s)^{1/2}\}/2K$$

$$b = 1 + KC_T + K[NP]/2n_s \quad (2)$$

where K is the intrinsic binding constant of the 3+ species, n_s is the number of pairs required per $Co(phen)_3^{3+}$, and [NP] is the nucleotide phosphate concentration. Equation 2 is valid for noncooperative, nonspecific binding with the existence of one type of discreet binding site. An analogous treatment could be used for a more complicated type of binding interaction.[17] The small viscosity changes that occur upon addition of the metal ion solution are also neglected. A regression analysis of the data in Figure 2 to eq 1 and 2 yield the following: $K = 5.8 \times 10^3$ M^{-1}, $n_s = 6.7$ base pairs, $D_f = 4.1 \times 10^{-6}$ cm^2/s, $D_b = 1.2 \times 10^{-7}$ cm^2/s. The value for n_s found here is somewhat larger than that reported for $Ru(phen)_3^{2+}$ ($n_s = 4$ bp). K is close to that for the $Ru(phen)_3^{2+}$ ($K = 6.2 \times 10^3$ M^{-1}).[1a] The positive 40-mV shift in the peak potential for bound complex compared to free $Co(phen)_3^{3+}$ unequivocally shows the +2 species (binding constant, K') is bound more strongly than the +3 species with $K'/K = 4.8$; $K' = 2.8 \times 10^4$ M^{-1}. This stronger binding of +2 might be explained by the importance of hydrophobic interactions, in addition to electrostatic ones.[1f,g] Similar effects have been found, for example, in the interaction of viologens and metal chelates with micelles[18] and perfluorosulfonated (Nafion) films.[19]

The results given here demonstrate that rather straightforward electrochemical methods can be employed to characterize the intercalative interaction between a metal complex or other electroactive species and DNA to yield estimates of the binding constants and binding site sizes. The electrochemical oxidation and reduction of selected bound species on DNA can also be carried out and in favorable circumstances may allow chemical changes in the DNA, e.g., strand scission.

Acknowledgment. The support of this research by the National Science Foundation (CHE 8304666) is gratefully acknowledged. We thank P. Vanderslice and W. Copeland for many helpful discussions and assistance with gel electrophoresis.

Registry No. $Co(phen)_3^{3+}$, 18581-79-8.

(14) Concentrations of nucleotide phosphate were determined spectrophotometrically on dilution with $\epsilon_{260} = 6600$ M^{-1} cm^{-1} (Reichmann, M. E.; Rice, S. A.; Thomas, C. A.; Doty, P. *J. Am. Chem. Soc.* **1954**, *76*, 3047. The molecular weight of our DNA was ca. 5.1×10^6 (ca. 6600 bp) based upon gel electrophoresis. This is approximately 85% of the MW of calf thymus DNA given in ref 15.

(15) Tanford, C. *Physical Chemsitry of Macromolecules*; Wiley, New York: 1963; p 361.

(16) Bard, A. J.; Faulkner, L. R. *Electrochemical Methods*; Wiley: New York, 1980; Chapter 6.

(17) McGhee, J. D.; von Hippel, P. H. *J. Mol. Biol.* **1974**, *86*, 469.

(18) (a) +1 vs +2 species of 1-decyl-1′-methyl-4,4′-bipyridinium in Triton X-100: Hoshino, K.; Sasaki, H.; Suga, K.; Saji, T. *Bull. Chem. Soc. Jpn.* **1987**, *60*, 1521. (b) +1 vs +2 of methyl viologen in SDS micelles: Kaifer, A. E.; Bard, A. J. *J. Phys. Chem.* **1985**, *89*, 4876. (c) $Os(bpy)_3^{2+}$ vs $Os(bpy)_3^{3+}$ in SDS micelles: Ouyang, J.; Bard, A. J. *Bull. Chem. Soc. Jpn.*, in press.

(19) $Ru(bpy)_3^{2+}$ vs $Ru(bpy)_3^{3+}$ in Nafion: Martin, C. R.; Rubinstein, I.; Bard, A. J. *J. Am. Chem. Soc.* **1982**, *104*, 4817.

2-Deoxy-2-fluoroglucosides: A Novel Class of Mechanism-Based Glucosidase Inhibitors

Stephen G. Withers,* Ian P. Street, Paul Bird, and David H. Dolphin

Department of Chemistry
University of British Columbia
Vancouver, British Columbia, Canada V6T 1Y6

Received July 2, 1987

Glucosidase inhibitors are of interest in the treatment of diabetes and obesity due to their potential in controlling blood glucose levels.[1] Currently available glucosidase inhibitors include the noncovalent, naturally occurring inhibitors such as acarbose[2] and nojirimycin[3] and covalent, mechanism-based inhibitors such as the conduritol epoxides[4] and glucosylmethyltriazenes.[5] This paper describes a novel mechanism-based glucosidase inhibitor based on a strategy which has not previously been exploited for this class of enzymes.

The enzymic hydrolysis of glucosidases likely proceeds through a glucosyl enzyme intermediate via oxocarbonium ion-like transition states as shown in Scheme I.[6] Therefore substitution of an electronegative fluorine atom for a hydroxyl group adjacent to the reaction center, at C-2, should destabilize these transition states and decrease both the rates of glycosylation (k_1) and deglycosylation (k_2). Indeed, we have synthesized several 2-deoxy-2-fluoroglucosides and glucosyl phosphates and found them to be very slow substrates for their respective glucosidases or glucosyl transferases, with K_m values generally similar to those for the normal substrate. A similar approach has been employed previously[7] in studies of terpene biosynthetic enzymes where reaction proceeds via carbocationic intermediates.

The incorporation of a highly reactive leaving group as the aglycone into such deactivated substrates might increase the glycosylation rate sufficiently to permit trapping of the 2-fluorodeoxyglucosyl enzyme intermediate, therefore inhibiting the enzyme in a temporary covalent fashion. We describe here the synthesis[8] and testing of such an inhibitor, 2,4-dinitrophenyl

(1) Truscheit, E.; Frommer, W.; Junge, B.; Müller, L.; Schmidt, D. D.; Wingender, W. *Angew. Chem., Int. Ed. Engl.* **1981**, *20*, 744.

(2) Schmidt, D. D.; Frommer, W.; Junge, B.; Müller, L.; Wingender, W.; Truscheit, E.; Schafer, D. *Naturwissenschaften* **1977**, *64*, 535.

(3) Schmidt D. D.; Frommer W.; Müller, L.; Truscheit, E. Naturwissenschaften 1979, 66, 584.

(4) Legler, G. *Methods Enzymol.* **1977**, *46*, 308.

(5) Marshall, P. J.; Sinnott, M. L.; Smith, P. J.; Widdows, D. *J. Chem. Soc., Perkin Trans. 1* **1981**, 366.

(6) Sinnott, M. L. *The Chemistry of Enzyme Action*; Elsevier: New York, 1984; pp 389-431.

(7) (a) Poulter, C. D.; Satterwhite, D. M. *Biochemistry* **1977**, *16*, 5470. (b) Poulter, C. D.; Wiggins, P. L.; Le, A. T. *J. Am. Chem. Soc.* **1981**, *103*, 3926. (c) Mash, E. A.; Gurria, G. M.; Poulter, C. D. *J. Am. Chem. Soc.* **1981**, *103*, 3927.

(8) Hydrolysis of 3,4,6-tri-*O*-acetyl-2-deoxy-2-fluoro-α-D-glucopyranosyl bromide[9] afforded the anomeric mixture of protected hemiacetals. Treatment of this mixture with 1-fluoro-2-4-dinitrobenzene in the presence of DABCO[10] gave a mixture of the α- and β-dinitrophenyl glycoside peracetates which was separated by fractional crystallization. Deprotection (NaOMe/MeOH) of the β-anomer afforded crystalline **1**. Satisfactory spectral and analytical data were obtained for all compounds.

0002-7863/87/1509-7530$01.50/0